PLOS ONE

RESEARCH ARTICLE

Peristaltic Transport of Prandtl-Eyring Liquid in a Convectively Heated Curved Channel

Tasawar Hayat[1,2], Shahida Bibi[1], Fuad Alsaadi[2], Maimona Rafiq[1]*

1 Department of Mathematics, Quaid-i-Azam University 45320, Islamabad 44000, Pakistan, **2** Department of Electrical and Computer Engineering, Faculty of Engineering, King Abdulaziz University, Jeddah 21589, Saudi Arabia

* maimona_88@hotmail.com

Abstract

Here peristaltic activity for flow of a Prandtl-Eyring material is modeled and analyzed for curved geometry. Heat transfer analysis is studied using more generalized convective conditions. The channel walls satisfy complaint walls properties. Viscous dissipation in the thermal equation accounted. Unlike the previous studies is for uniform magnetic field on this topic, the radial applied magnetic field has been utilized in the problems development. Solutions for stream function (ψ), velocity (u), and temperature (θ) for small parameter β have been derived. The salient features of heat transfer coefficient Z and trapping are also discussed for various parameters of interest including magnetic field, curvature, material parameters of fluid, Brinkman, Biot and compliant wall properties. Main observations of present communication have been included in the conclusion section.

Citation: Hayat T, Bibi S, Alsaadi F, Rafiq M (2016) Peristaltic Transport of Prandtl-Eyring Liquid in a Convectively Heated Curved Channel. PLoS ONE 11 (6): e0156995. doi:10.1371/journal.pone.0156995

Editor: Xiao-Dong Wang, North China Electric Power University, CHINA

Received: November 2, 2015

Accepted: May 23, 2016

Published: June 15, 2016

Data Availability Statement: All relevant data are within the paper.

Funding: The authors received no specific funding for this work.

Competing Interests: The authors have declared that no competing interests exist.

Introduction

Peristaltic transport holds a considerable position in physiology and engineering. Extensive research has been addressed under different situations since the seminal works of Latham [1] and Shapiro et al. [2]. Locomotion of worm, gliding movement of some bacteria, corrosive and sanitary liquids transport, heart lung machine and roller and finger pumps also uses this mechanism for their working. Heat transfer in peristalsis is further significant in chemical and pharmaceutical industries, hemodialysis, oxygenation, tissue analysis, thermotherapy and human thermoregulatory process. Heat transfer is also quite prevalent in several peristaltic pumps. Gul et al. [3] discussed the effect of temperature dependent viscosity on the flow of third grade fluid over vertical belt. Gul et al. [4, 5] also study the heat transfer analysis by considering oscillating vertical and inclined belt. Besides this, advancement is also made about the interaction of magnetohydrodynamics in peristalsis, which finds great importance in connection with certain problems for motion of conductive fluids in physiology, for instance, the blood and blood pumps machines, hyperthermia, cancer therapy, drug delivery transport, magnetic resonance imaging (MRI) and theoretical research about operation of peristaltic magnetohydrodynamic (MHD) compressors. Motivated by all the aforementioned facts the recent investigators are

also engaged in the analysis of peristalsis through diverse aspects. Few recent studies and several interesting references in this direction can be seen in the attempts [6–21].

All the aforementioned attempts and existing information on this topic witness that much attention has been given to the flows with peristalsis in a planer channel which seems inadequate in reality. It is because of the fact that most of the ducts in physiological and industrial applications are curved. Influence curvature on peristaltic transport liquid is discussed in only some studies. Sato et al. [22] initially examined the curvature effect in the peristalsis of viscous fluid. Ali et al. [23] reconsidered the problem of ref [24] in wave frame. Hayat et al. [25] study the peristaltic phenomenon for viscous fluid in curved geometry. The peristaltic flow of third order and Carreau-Yasuda materials in curved flow configuration has been discussed by Ali et al. [26] and Abbasi et al. [27] respectively. Heat/mass transport in peristalsis of pseudoplastic, Johnson-Segalman and third grade fluids are explored by Hina et al. [28–29] and Hayat et al. [30]. On the other hand it has also been noted that heat transfer in previous studies related to peristalsis has been dealt with either prescribing temperature or heat flux at the channel walls. Scarce information is available for peristalsis involving heat transfer through convective conditions (see [31–33]).

The facts of present attempt is to advance the theory of peristalsis of non-Newtonian materials via three important aspects i.e. curved channel, convective heat transfer condition and radial magnetic field. Hence we model here the governing flow problem employing constitutive relations of Prandtl-Eyring fluid. The flow formulation is completed through compliant properties of channel walls. Arising nonlinear analysis is computed for the series solutions. Arrangement of paper is as follows. Next section formulates the problems for flow and temperature. Section three includes solution expressions for the stream function, temperature and heat transfer coefficient. Discussion to graph of different physical quantities for various parameters is assigned in section four. section five consists of conclusions.

Formulation

Consider a channel in curved shape with width $2d_1$ looped in a circle with radius R^* and center O (see Fig 1). Coordinate axis are selected in such a way that x-axis lies along the length of the channel and r-axis lies normal to it. An incompressible electrically conducting Prandtl-Eyring fluid fills the channel. Flow in the channel is generated by propagating peristaltic waves along the channel walls in the axial direction with constant speed c. A radial magnetic field $\mathbf{B} = (\frac{B_0}{r+R^*}, 0, 0)$ is applied. Induced magnetic field is neglected for small magnetic Reynolds number assumption. Electric field is further absent.

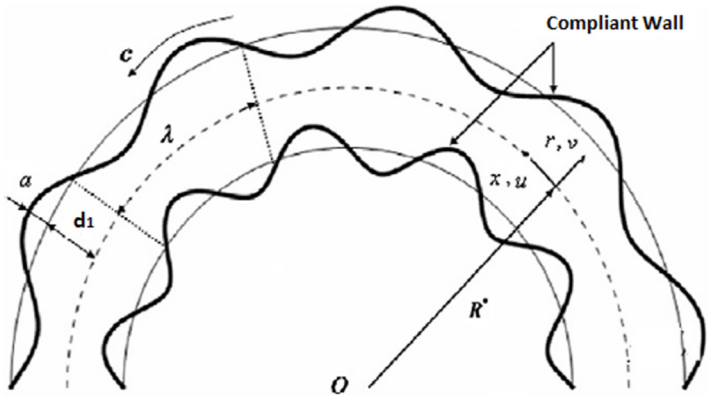

Fig 1. Geometry of the problem.

doi:10.1371/journal.pone.0156995.g001

The wave form at the walls are

$$r = \pm\eta(\mathrm{x}, \mathrm{t}) = \pm\left[\mathrm{d}_1 + \mathrm{asin}\left(\frac{2\pi}{\lambda}(\mathrm{x} - \mathrm{ct})\right)\right], \tag{1}$$

here *a* depicts the wave amplitude, λ the wavelength and t the time. The constitutive equations are:

$$\frac{\partial[(r+R^*)v]}{\partial r} + R^*\frac{\partial u}{\partial x} = 0, \tag{2}$$

$$\rho\left(\frac{\partial v}{\partial t} + v\frac{\partial v}{\partial r} + \frac{R^*u}{r+R^*}\frac{\partial v}{\partial x} - \frac{u^2}{r+R^*}\right) = -\frac{\partial p}{\partial r} + \frac{1}{r+R^*}\frac{\partial[(r+R^*)S_{rr}]}{\partial r} + \frac{R^*}{r+R^*}\frac{\partial S_{xr}}{\partial x} - \frac{S_{xx}}{r+R^*} - \frac{\sigma v B_0^2}{(r+R^*)^2}, \tag{3}$$

$$\rho\left(\frac{\partial u}{\partial t} + v\frac{\partial u}{\partial r} + \frac{R^*u}{r+R^*}\frac{\partial u}{\partial x} + \frac{uv}{r+R^*}\right) = -\frac{R^*u}{r+R^*}\frac{\partial p}{\partial x} + \frac{1}{(r+R^*)^2}\frac{\partial[(r+R^*)^2 S_{rx}]}{\partial r} + \frac{R^*}{r+R^*}\frac{\partial S_{xx}}{\partial x} - \frac{\sigma u B_0^2}{(r+R^*)^2}, \tag{4}$$

$$\rho C_p\left(\frac{\partial T}{\partial t} + v\frac{\partial T}{\partial r} + \frac{R^*u}{r+R^*}\frac{\partial T}{\partial x}\right) = \kappa\left(\frac{\partial^2 T}{\partial r^2} + \frac{1}{r+R^*}\frac{\partial T}{\partial r} - \left(\frac{R^*}{r+R^*}\right)^2\frac{\partial^2 T}{\partial x^2}\right) + (S_{rr} - S_{xx})\left(\frac{\partial v}{\partial r}\right) + S_{xr}\left(\frac{\partial u}{\partial r} + \frac{R^*}{r+R^*}\frac{\partial v}{\partial x} - \frac{u}{r+R^*}\right), \tag{5}$$

where σ is the electrical conductivity of fluid, S_{ij} $(i, j = r, x)$ the components of extra stress tensor, C_p denotes the specific heat, ρ the density, κ stands for thermal conductivity and T the temperature of fluid.

Extra stress tensor **(S)** for Prandtl-Eyring fluid is written as:

$$\mathbf{S} = \frac{1}{\dot{\gamma}}A\sinh^{-1}\left(\frac{\dot{\gamma}}{C}\right)\mathbf{A_1}, \tag{6}$$

$$\dot{\gamma} = \sqrt{\frac{1}{2}\Pi}, \tag{7}$$

$$\Pi = tr(\boldsymbol{A}_1)^2,$$

$$A_1 = \mathbf{L} + \mathbf{L}^{transpose},$$

where $\mathbf{L}$ = (grad $\mathbf{V}$) and A/C are material constants of Prandtl-Eyring fluid model.

The boundary conditions have been assumed in the form

$$u = 0 \; at \; r = \pm\eta \tag{8}$$

$$k\frac{\partial T}{\partial r} = -h_1(T - T_0) \; at \; r = +\eta, \tag{9}$$

$$k\frac{\partial T}{\partial r} = -h_1(T_0 - T)\ at\ r = -\eta, \tag{10}$$

$$R^*\left[-\tau\frac{\partial^3\eta}{\partial x^3} + \mathrm{m}_1\frac{\partial^3\eta}{\partial x\partial t^2} + \mathrm{d}\frac{\partial^2\eta}{\partial t\partial x}\right] = \frac{1}{(r+R^*)}\frac{\partial[(r+R^*)^2 S_{rx}]}{\partial r} + \frac{\partial S_{xx}}{\partial x} - \rho(r+R^*)\left(\frac{\partial u}{\partial t} + v\frac{\partial u}{\partial r} + \frac{R^* u}{r+R^*}\frac{\partial u}{\partial x} + \frac{uv}{r+R^*}\right) - \frac{\sigma u B_0^2}{(r+R^*)^2}\ at\ r = \pm\eta. \tag{11}$$

Here T_0 is the temperature at both upper and lower walls of the channel, h_1 the heat transfer coefficient at upper/lower walls whereas S_{xx}, S_{rr}, S_{rx} and S_{xr} are the elements of **S**. Moreover

$$L = -\tau\frac{\partial^2}{\partial x^2} + \mathrm{m}_1\frac{\partial^2}{\partial t^2} + \mathrm{d}\frac{\partial}{\partial t}, \tag{12}$$

where m_1, τ and d are the mass per unit area, longitudinal tension and the viscous damping coefficient respectively. Having

$$x^* = \frac{x}{\lambda},\ r^* = \frac{r}{d_1},\ p^* = \frac{d_1^2 p}{c\mu\lambda}, t^* = \frac{ct}{\lambda},\ u^* = \frac{u}{c},\ v^* = \frac{v}{c},$$

$$\boldsymbol{S}^* = \frac{\boldsymbol{dS}}{\mu c}, h = \frac{\eta}{d_1}, \mathrm{K} = \frac{R^*}{d_1}, \delta = \frac{d_1}{\lambda}, \theta = \frac{T - T_0}{T_0}.$$

Eqs (3)–(11) can be reduced as follows:

$$Re\delta\left[\delta\frac{\partial v}{\partial t} + v\frac{\partial v}{\partial r} + \frac{\mathrm{K}\delta u}{(r+\mathrm{K})}\frac{\partial v}{\partial x} - \frac{u^2}{(r+\mathrm{K})}\right] = -\frac{\partial p}{\partial r} + \delta\left[\frac{1}{(r+\mathrm{K})}\frac{\partial}{\partial r}[(r+\mathrm{K})S_{rr}] + \frac{\mathrm{K}\delta}{(r+\mathrm{K})}\frac{\partial}{\partial x}S_{xr} - \frac{S_{xx}}{(r+\mathrm{K})}\right], \tag{13}$$

$$-Re\left[\delta\frac{\partial u}{\partial t} + v\frac{\partial u}{\partial r} + \frac{\mathrm{K}\delta u}{(r+\mathrm{K})}\frac{\partial u}{\partial x} + \frac{uv}{(r+\mathrm{K})}\right] = -\frac{\mathrm{K}}{(r+\mathrm{K})}\frac{\partial p}{\partial x} + \frac{1}{(r+\mathrm{K})^2}\frac{\partial}{\partial r}[(r+\mathrm{K})^2 S_{rx}] + \frac{\mathrm{K}\delta}{(r+\mathrm{K})}\frac{\partial}{\partial x}S_{xx} - \frac{H^2 u}{(r+\mathrm{K})^2}, \tag{14}$$

$$Re\left[\delta\frac{\partial}{\partial t} + v\frac{\partial}{\partial r} + \frac{\mathrm{K}\delta u}{(r+\mathrm{K})}\frac{\partial}{\partial x}\right]\theta = \frac{1}{Pr}\left[\frac{\partial^2}{\partial r^2} + \frac{1}{(r+\mathrm{K})}\frac{\partial}{\partial r} + \delta^2\frac{\partial^2}{\partial x^2}\right]\theta + Ec\left[(S_{rr} - S_{xx})\frac{\partial v}{\partial r} + S_{xr}\left(\frac{\partial u}{\partial r} + \frac{\mathrm{K}\delta}{(r+\mathrm{K})}\frac{\partial v}{\partial x} - \frac{u}{(r+\mathrm{K})}\right)\right], \tag{15}$$

with the following non-dimensional boundary conditions

$$u = 0\ at\ r = \pm h, \tag{16}$$

$$\frac{\partial\theta}{\partial r} + Bi_1\theta = 0\ at\ r = h, \tag{17}$$

$$\frac{\partial\theta}{\partial r} - Bi_1\theta = 0\ at\ r = -h, \tag{18}$$

$$\left[E_1\frac{\partial^3 h}{\partial x^3}+E_2\frac{\partial^3 h}{\partial x\partial t^2}+E_3\frac{\partial^2 h}{\partial t\partial x}\right]=-\frac{Re(r+\mathrm{K})}{K}\left[\delta\frac{\partial u}{\partial t}+v\frac{\partial u}{\partial r}+\frac{\mathrm{K}\delta}{(r+\mathrm{K})}\frac{\partial u}{\partial x}+\frac{uv}{(r+\mathrm{K})}\right]$$
$$+\frac{1}{\mathrm{K}(r+\mathrm{K})}\frac{\partial}{\partial r}[(r+\mathrm{K})^2 S_{rx}]+\frac{\delta}{\mathrm{K}}\frac{\partial S_{xx}}{\partial x}-\frac{H^2 u}{\mathrm{K}(r+\mathrm{K})^2}\ at\ r=\pm h, \quad (19)$$

with $$h=\pm[1+\epsilon sin2\pi(x-t)].$$

Taking the stream function $\psi\ (x, r, t)$ by

$$u=-\frac{\partial\psi}{\partial r}\ , v=\delta\frac{\mathrm{K}}{(r+\mathrm{K})}\frac{\partial\psi}{\partial x}. \quad (20)$$

Eq (2) is identically satisfied and Eqs (13)–(19) after utilizing lubrication approximation take the forms:

$$\frac{\partial p}{\partial r}=0, \quad (21)$$

$$-\frac{\mathrm{K}}{(r+\mathrm{K})}\frac{\partial p}{\partial x}+\frac{1}{(r+\mathrm{K})^2}\frac{\partial}{\partial r}[(r+\mathrm{K})^2 S_{rx}]+\frac{H^2\psi_r}{(r+\mathrm{K})^2}=0, \quad (22)$$

$$\left[\frac{\partial^2}{\partial r^2}+\frac{1}{(r+\mathrm{K})}\frac{\partial}{\partial r}\right]\theta=-Br\left[S_{xr}\left(-\psi_{rr}+\frac{\psi_r}{(r+\mathrm{K})}\right)\right], \quad (23)$$

$$\psi_r=0\ at\ r=\pm h, \quad (24)$$

$$\frac{\partial\theta}{\partial r}+Bi_1\theta=0\ at\ r=h, \quad (25)$$

$$\frac{\partial\theta}{\partial r}-Bi_1\theta=0\ at\ r=-h, \quad (26)$$

$$\left[E_1\frac{\partial^3}{\partial x^3}+E_2\frac{\partial^3}{\partial x\partial t^2}+E_3\frac{\partial^2}{\partial t\partial x}\right]h=\frac{1}{\mathrm{K}(r+\mathrm{K})}\frac{\partial}{\partial r}[(r+k)^2 S_{rx}]+\frac{H^2\psi_r}{\mathrm{K}(r+\mathrm{K})^2}\ at\ r=\pm h, \quad (27)$$

where $\epsilon\ (=a/d_1)$, $\delta\ (=d_1/\lambda)$ and K represent the dimensionless amplitude ratio, wave number and curvature parameter respectively. $E_1=-\frac{\tau d_1^3}{\lambda_1^3\mu c}$, $\mathrm{E}_2=\frac{m_1 c d_1^3}{\lambda_1^3\mu c}$, $\mathrm{E}_3=\frac{dd_1^3}{\lambda_1^2\mu}$ the non-dimensional elasticity parameters, Re $(=cd_1/\nu)$ depicts the Reynolds number, $Pr\ (=\mu C_p/\kappa)$ the Prandtl number, $We\ (=mc/d_1)$ the Weissenberg number, $H(=B_0 d\sqrt{\sigma/\mu})$ the Hartman number, $Ec\ (=c^2/C_pT_0)$ the Eckert number, $Br\ (=EcPr)$ the Brinkman number and $Bi_1\ (=h_1/d)$ the Biot number. Further the dimensionless form of extra stress tensor after invoking long wavelength and low Reynolds number approximation becomes

$$S_{rx}=\alpha\left(-\psi_{rr}+\frac{\psi_r}{(r+\mathrm{K})}\right)-\frac{\beta}{6}\left(-\psi_{rr}+\frac{\psi_r}{(r+\mathrm{K})}\right)^3, \quad (28)$$

with $\alpha=\frac{A}{\mu C}$ and $\beta=\frac{\alpha c^2}{C^2 d_1^2}$. Heat transfer coefficient is given by

$$Z=h_x\theta_r(h).$$

Solution Methodology

The governing equations are highly non-linear and exact solution seems impossible. Therefore, perturbation method for small parameter β is used to find the solution. Thus we expand ψ, S_{rx}, θ and Z as follows:

$$\psi = \psi_0 + \beta\psi_1 + \dots , \tag{29}$$

$$S_{rx} = S_{0rx} + \beta S_{1rx} + \dots , \tag{30}$$

$$\theta = \theta_0 + \beta\theta_1 + \dots , \tag{31}$$

$$Z = Z_0 + \beta Z_1 + \dots , \tag{32}$$

Zeroth order system and solution

Using eqs (29)–(32) into eqs (21)–(28) and comparing the coefficients of β^0 we have

$$\frac{\partial}{\partial r}\left[\frac{1}{\mathrm{K}(r+\mathrm{K})}\frac{\partial}{\partial r}[(r+\mathrm{K})^2 S_{0rx}] + \frac{H^2\psi_{0r}}{\mathrm{K}(r+\mathrm{K})}\right] = 0, \tag{33}$$

$$\left[\frac{\partial^2}{\partial r^2} + \frac{1}{(r+\mathrm{K})}\frac{\partial}{\partial r}\right]\theta_0 = -Br\left[S_{0xr}\left(-\psi_{0rr} + \frac{\psi_{0r}}{(r+\mathrm{K})}\right)\right], \tag{34}$$

$$\psi_{0r} = 0 \; at \; r = \pm h \, , \tag{35}$$

$$\frac{\partial\theta_0}{\partial r} + Bi_1\theta_0 = 0 \; at \; r = h, \tag{36}$$

$$\frac{\partial\theta_0}{\partial r} - Bi_1\theta_0 = 0 \; at \; r = -h, \tag{37}$$

$$\left[E_1\frac{\partial^3 h}{\partial x^3} + E_2\frac{\partial^3 h}{\partial x\partial t^2} + E_3\frac{\partial^2 h}{\partial t\partial x}\right] = \frac{1}{\mathrm{K}(r+\mathrm{K})}\frac{\partial}{\partial r}[(r+\mathrm{K})^2 S_{0rx}] + \frac{H^2\psi_{0r}}{\mathrm{K}(r+\mathrm{K})^2} \; at \; r = \pm h, \tag{38}$$

with

$$S_{0rx} = \left(-\psi_{0rr} + \frac{\psi_{0r}}{(r+\mathrm{K})}\right).$$

Solving the above system we get

$$\psi_0 = \frac{\sqrt{\alpha}(r+\mathrm{K})^{\frac{1+\sqrt{H^2+\alpha}}{\sqrt{\alpha}}}}{\sqrt{H^2+\alpha}+\sqrt{\alpha}}\mathrm{C}_1 - \frac{\sqrt{\alpha}(r+\mathrm{K})^{\frac{1-\sqrt{H^2+\alpha}}{\sqrt{\alpha}}}}{\sqrt{H^2+\alpha}-\sqrt{\alpha}}\mathrm{C}_2 + r(r+\mathrm{K})C_3 + C_4, \tag{39}$$

$$\theta_0 = B_2 + \frac{1}{4}\left[-Br(r+\mathrm{K})^{\frac{-2\sqrt{H^2+\alpha}}{\sqrt{\alpha}}}\alpha\left((r+\mathrm{K})^{\frac{4\sqrt{H^2+\alpha}}{\sqrt{\alpha}}}B_{15} + B_{16}\right) + 4B_1\ln(r+\mathrm{K}) + 4BrB_{17}H^2(\ln(r+\mathrm{K}))^2\right], \tag{40}$$

and heat transfer coefficient is given by

$$Z_0 = h_x[2B_1 + Br(h+\mathrm{K})\frac{-2\sqrt{H^2+\alpha}}{\sqrt{\alpha}}\left(B_{13} - B_{14}(\mathrm{K}+h)\frac{4\sqrt{H^2+\alpha}}{\sqrt{\alpha}}\right)\sqrt{\alpha}\,\sqrt{H^2+\alpha} + 8BrB_{17}H^2\ln(\mathrm{K}+h)/(\mathrm{K}+h)]. \quad (41)$$

First order system and solution

$$\frac{\partial}{\partial r}\left[\frac{1}{\mathrm{K}(r+\mathrm{K})}\frac{\partial}{\partial r}[(r+\mathrm{K})^2 S_{1rx}] + \frac{H^2\psi_{1r}}{\mathrm{K}(r+\mathrm{K})}\right] = 0, \quad (42)$$

$$\left[\frac{\partial^2}{\partial r^2} + \frac{1}{(r+\mathrm{K})}\frac{\partial}{\partial r}\right]\theta_1 = -Br\left[S_{1xr}\left(-\psi_{0rr} + \frac{\psi_{0r}}{(r+\mathrm{K})}\right) + S_{0xr}\left(-\psi_{1rr} + \frac{\psi_{1r}}{(r+\mathrm{K})}\right)\right], \quad (43)$$

$$\psi_{1r} = 0 \; at \; r = \pm h\,, \quad (44)$$

$$\frac{\partial\theta_1}{\partial r} + Bi_1\theta_1 = 0 \; at \; r = h\,, \quad (45)$$

$$\frac{\partial\theta_1}{\partial r} + Bi_1\theta_1 = 0 \; at \; r = -h\,, \quad (46)$$

$$\frac{1}{(r+\mathrm{K})}\frac{\partial}{\partial r}[(r+\mathrm{K})^2 S_{1rx}] + \frac{H^2\psi_{1r}}{(r+\mathrm{K})^2} = 0 \; at \; r = \pm h, \quad (47)$$

with

$$S_{1rx} = \alpha\left(-\psi_{0rr} + \frac{\psi_{0r}}{r+\mathrm{K}}\right) - \frac{\beta}{6}\left(-\psi_{0rr} + \frac{\psi_{0r}}{(r+\mathrm{K})}\right)^3. \quad (48)$$

The results corresponding to first order system are

$$\psi_1 = -C_1^2C_2H^2(\mathrm{K}+r)\frac{-1+\sqrt{H^2+\alpha}}{\sqrt{\alpha}}C_9 + C_2^2C_1H^2(\mathrm{K}+r)\frac{-1-\sqrt{H^2+\alpha}}{\sqrt{\alpha}}C_{10} + C_1^3(\mathrm{K}+r)\frac{-1+3\sqrt{H^2+\alpha}}{\sqrt{\alpha}} \times C_{11} - C_2^3(\mathrm{K}+r)\frac{-1-3\sqrt{H^2+\alpha}}{\sqrt{\alpha}}C_{12} + (\mathrm{K}+r)\frac{\sqrt{H^2+\alpha}}{\sqrt{\alpha}}(\mathrm{K}\sqrt{\alpha}C_{13} + r\sqrt{\alpha}C_{14})C_5 + (\mathrm{K}+r)\frac{-\sqrt{H^2+\alpha}}{\sqrt{\alpha}} \times (\mathrm{K}\sqrt{\alpha}C_{15} + r\sqrt{\alpha}C_{16})C_6 + \mathrm{K}rC_7 + \frac{1}{2r^2C_7} + C_8, \quad (49)$$

$$\theta_1 = 1/96[\frac{6BrC_1^2C_2^2H^4}{(\mathrm{K}+r)^2\alpha^2} + BrC_1^4H^2(\mathrm{K}+r)\frac{-2+4\sqrt{H^2+\alpha}}{\sqrt{\alpha}}B_7 - BrC_2^4H^2(\mathrm{K}+r)\frac{-2-4\sqrt{H^2+\alpha}}{\sqrt{\alpha}}B_8 + 4(\mathrm{K}+r)\frac{2\sqrt{H^2+\alpha}}{\sqrt{\alpha}}\left(B_9 + \frac{B_{10}}{(\mathrm{K}+r)^2}\right) + 4(\mathrm{K}+r)\frac{-2\sqrt{H^2+\alpha}}{\sqrt{\alpha}}\left(B_{11} + \frac{B_{12}}{(\mathrm{K}+r)^2}\right) + 96B_4 \; 96B_3\log(\mathrm{K}+r) + 48Br(C_2C_5 + C_1(2C_2+C_6))H^2\log(\mathrm{K}+r)^2], \quad (50)$$

and heat transfer coefficient is given by

$$Z_1 = \frac{1}{96(\mathrm{K}+h)^3}h_x\Bigg[(96B_3(\mathrm{K}+h)^2 - 8B_{12}(\mathrm{K}+h)\frac{-2\sqrt{H^2+\alpha}}{\sqrt{\alpha}} - 8B_{10}(\mathrm{K}+h)\frac{2\sqrt{H^2+\alpha}}{\sqrt{\alpha}} - \frac{BrC_1^2}{\alpha^2}C_2^2H^4$$
$$+\frac{1}{\sqrt{\alpha}}\Bigg\{-8(\mathrm{K}+h)\frac{-2\sqrt{H^2+\alpha}}{\sqrt{\alpha}}(B_{11}(\mathrm{K}+h)^2+B_{12})\sqrt{H^2+\alpha}$$
$$+8(\mathrm{K}+h)\frac{2\sqrt{H^2+\alpha}}{\sqrt{\alpha}}(B_9(\mathrm{K}+h)^2+B_{10})\sqrt{H^2+\alpha}\Bigg\} \tag{51}$$
$$-BrC_2^4H^2(\mathrm{K}+h)\frac{-4\sqrt{H^2+\alpha}}{\sqrt{\alpha}}B_8\left(-2-\frac{4\sqrt{H^2+\alpha}}{\sqrt{\alpha}}\right)$$
$$+96Br(C_2C_5+C_1(2C_2+C_6))H^2(\mathrm{K}+h)^2\log(\mathrm{K}+h)$$
$$+BrC_1^4H^2B_7(\mathrm{K}+h)\frac{4\sqrt{H^2+\alpha}}{\sqrt{\alpha}}B_8\left(-2+\frac{4\sqrt{H^2+\alpha}}{\sqrt{\alpha}}\right)\Bigg].$$

Here the algebraic values of $C_1 \rightarrow C_6$ and $B_1 \rightarrow B_{12}$ can be evaluated using MATHEMATICA.

Results and Discussion

This portion analyzes the impact of several parameters of interest on the velocity (u), temperature distribution (θ), heat transfer coefficient (Z) and stream function (ψ).

Figs 2–6 are prepared to study velocity profile. It is shown by these figures that velocity profile is parabolic in nature. Also, maximum value is observed at the center of channel. Fig 2

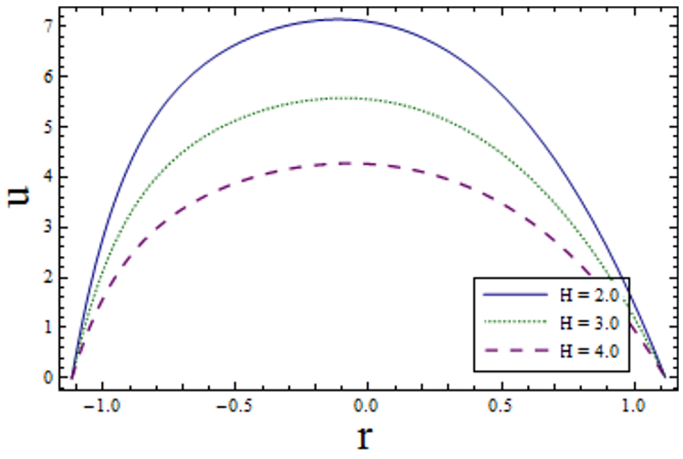

Fig 2. Variation of *H* on *u* when ϵ = 0.2, x = 0.2, t = 0.1, E_1 = 0.2, E_2 = 0.01, E_3 = 0.1, k = 3.5, α = 1.5 and β = 0.2.

doi:10.1371/journal.pone.0156995.g002

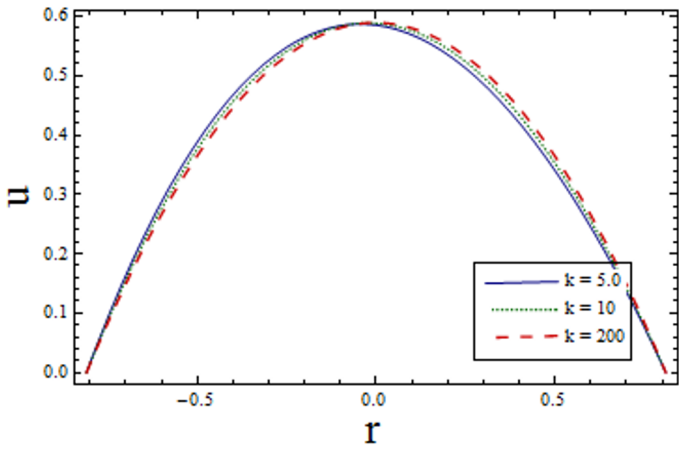

Fig 3. Variation of *k* on *u* when $\epsilon = 0.2$, x = 0.2, t = 0.1, $E_1 = 0.02$, $E_2 = 0.01$, $E_3 = 0.3$, H = 0.2, α = 1.5 and β = 0.2.

doi:10.1371/journal.pone.0156995.g003

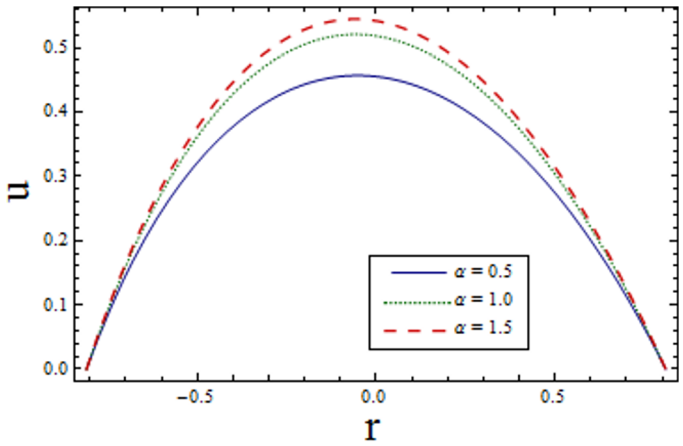

Fig 4. Variation of *α* on *u* when $\epsilon = 0.2$, x = 0.2, t = 0.1, $E_1 = 0.04$, $E_2 = 0.03$, $E_3 = 0.1$, k = 3.5, H = 2.5 and β = 0.2.

doi:10.1371/journal.pone.0156995.g004

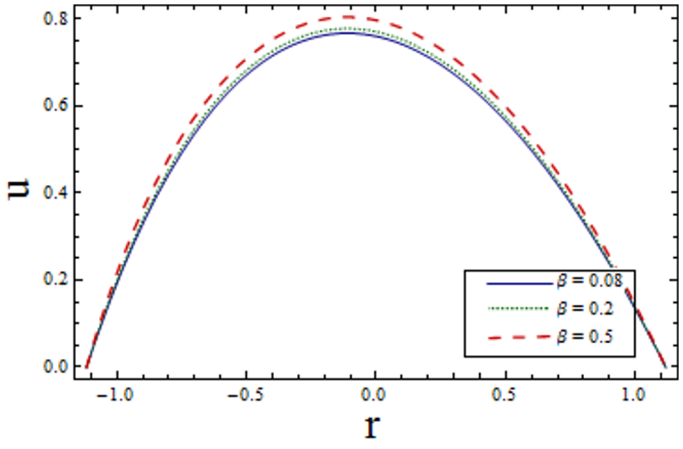

Fig 5. Variation of *β* on *u* when $\epsilon = 0.2$, x = 0.2, t = 0.1, $E_1 = 0.04$, $E_2 = 0.03$, $E_3 = 0.3$, k = 3.5, α = 1.5 and H = 2.0.

doi:10.1371/journal.pone.0156995.g005

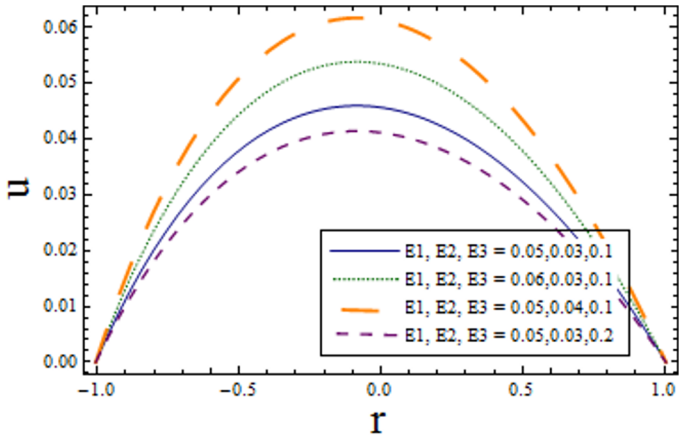

Fig 6. Variation of *complaint wall parameters* on *u* when $\epsilon = 0.2$, x = 0.2, t = 0.1, k = 3.5, α = 1.5, H = 2.8 and β = 0.2.

doi:10.1371/journal.pone.0156995.g006

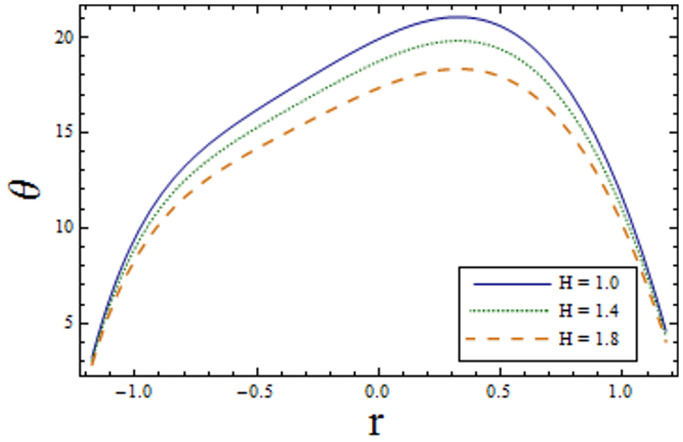

Fig 7. Variation of *H* on *θ* when $\epsilon = 0.2$, x = 0.3, t = 0.1, Br = 2, $E_1 = 0.04$, $E_2 = 0.03$, $E_3 = 0.02$, α = 1.5, β = 0.7, $Bi_1 = 10$ and k = 4.

doi:10.1371/journal.pone.0156995.g007

shows decrease in u by enhancing H. This is due to the fact that when the magnetic field is applied in the transverse direction, it provides resistance to the flow which in turn decreases the velocity. Fig 3 shows increase in the axial velocity u increases for larger curvature k near upper half of the channel. Whereas opposite behavior is seen near lower wall. Figs 4 and 5 indicate that the axial velocity acts like an increasing function of Prandtl Eyring fluid parameters α and β. Fig 6 illustrates that with an increase in E_1 and E_2 the velocity enhances. It is due to the fact that less resistance is offered to the flow because of the wall elastance and thus velocity increases. However reverse effect is observed for E_3. This is because of the fact that larger E_3 more resistive force due to damping and thus velocity decreases. Here we observe that the results obtained are in good agreement with the one get by Hina et al. [27].

Figs 7–13 indicate the effect of significant parameters involved in the temperature distribution θ. Fig 7 reveals that θ decreases when Hartman number H is increased. Fig 8 shows that increasing curvature K of the channel, we get opposite results for θ in upper/lower half of the channel. Figs 9 and 10 show that the temperature profile increases for larger Prandtl Eyring fluid parameters α and β. It is shown in Fig 11 that temperature increases via E_1 and E_2 and it

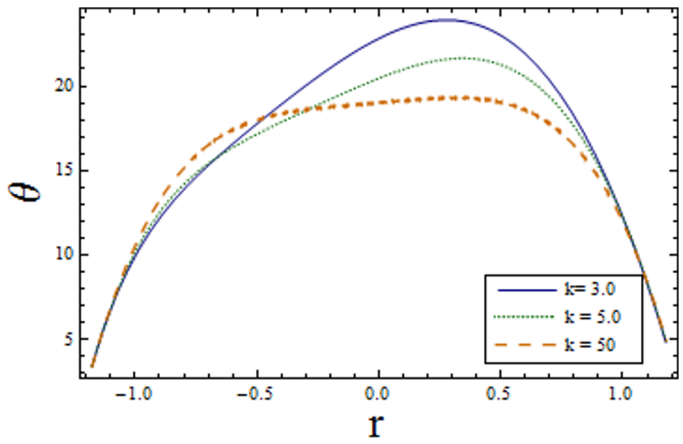

Fig 8. Variation of *k* on *θ* when $\epsilon = 0.2$, x = 0.3, t = 0.1, Br = 2, $E_1 = 0.04$, $E_2 = 0.03$, $E_3 = 0.02$, α = 1.5, β = 0.7, $Bi_1 = 10$ and k = 0.2.

doi:10.1371/journal.pone.0156995.g008

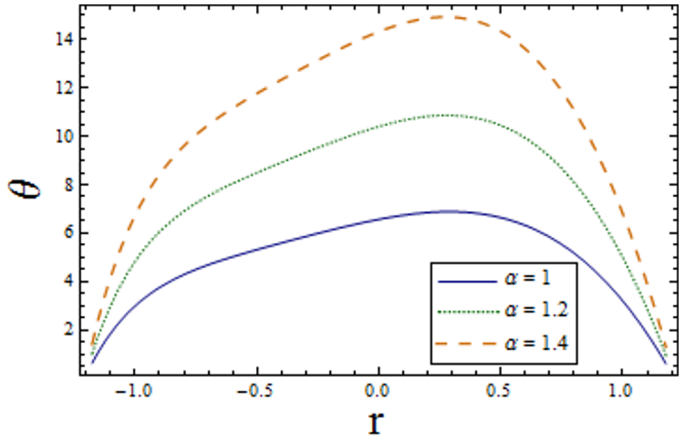

Fig 9. Variation of *α* on *θ* when $\epsilon = 0.2$, x = 0.3, t = 0.1, Br = 2, $E_1 = 0.04$, $E_2 = 0.03$, $E_3 = 0.01$, β = 0.7, H = 2.0, $Bi_1 = 10$ and k = 3.5.

doi:10.1371/journal.pone.0156995.g009

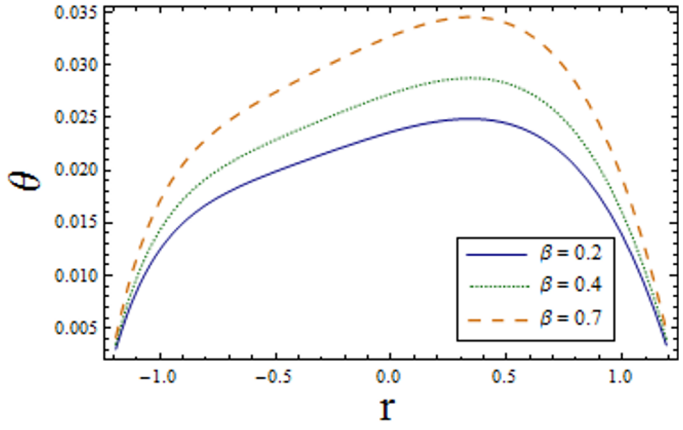

Fig 10. Variation of *β* on *θ* when $\epsilon = 0.2$, x = 0.3, t = 0.1, Br = 2, $E_1 = 0.04$, $E_2 = 0.03$, $E_3 = 0.01$, α = 1.5, H = 2.0, $Bi_1 = 10$ and k = 3.5.

doi:10.1371/journal.pone.0156995.g010

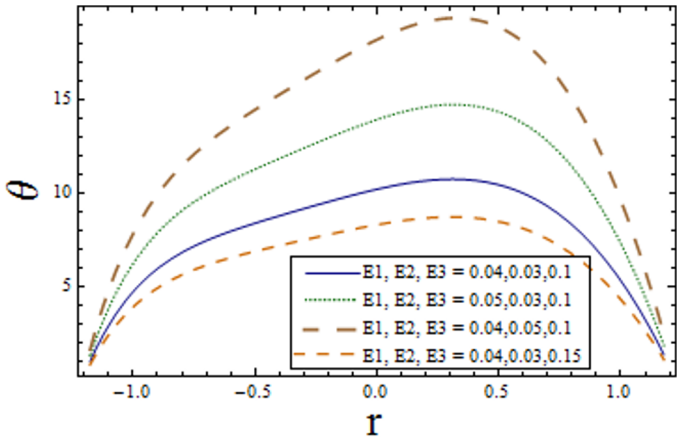

Fig 11. Variation of *complaint wall parameters* on θ when $\epsilon = 0.2$, x = 0.3, t = 0.1, Br = 2, $\beta = 0.7$, $\alpha = 1.5$, H = 2.0, $Bi_1 = 10$ and k = 3.5.

doi:10.1371/journal.pone.0156995.g011

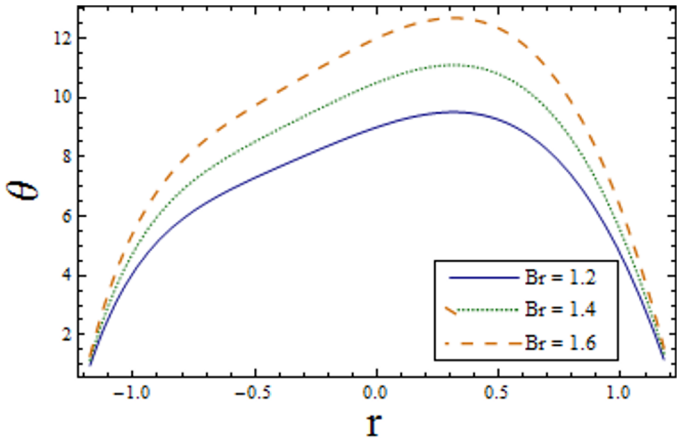

Fig 12. Variation of *Br* on θ when $\epsilon = 0.2$, x = 0.3, t = 0.1, $\beta = 0.7$, $E_1 = 0.04$, $E_2 = 0.03$, $E_1 = 0.01$, $\alpha = 1.5$, H = 2.0, $Bi_1 = 10$ and k = 3.5.

doi:10.1371/journal.pone.0156995.g012

decreases through E_3. Fig 12 illustrate that the temperature enhances when Brinkman number Br is increased. Fig 13 discloses that by increasing the Bi_1 the temperature decreases. Here we have considered the values of Biot number much larger than 0.1 due to non-uniform temperature fields within the fluid. Temperature is the average kinetic energy of the molecules. Increase/decrease in temperature directly effects the velocity. Therefore, we get almost similar qualitative behavior for velocity and temperature profiles.

In Figs 14–20 show the impact of various values of emerging parameters of Z(x). Fig 14 portrays that magnitude of Z(x) decreases when Hartman number H is increased. Fig 15 shows that the Z(x) increases when curvature parameter K is increased. The magnitude of Z(x) increases for larger Prandtl Eyring fluid parameters α and β (Figs 16 and 17). Fig 18 depicts that absolute value of Z(x) increases when there is an increase in E_1 and E_2. However heat transfer coefficient decreases for E_3. Fig 19 illustrates that absolute value of heat transfer coefficient enhances by increasing Br. Further $Z(x)$ is increasing function of Bi_1 (Fig 20).

Figs (21–25) display the streamline pattern for various values of invoked parameters. Fig 21a and 21b discusses the impact of Hartman number H on streamlines. Decrease in the size is

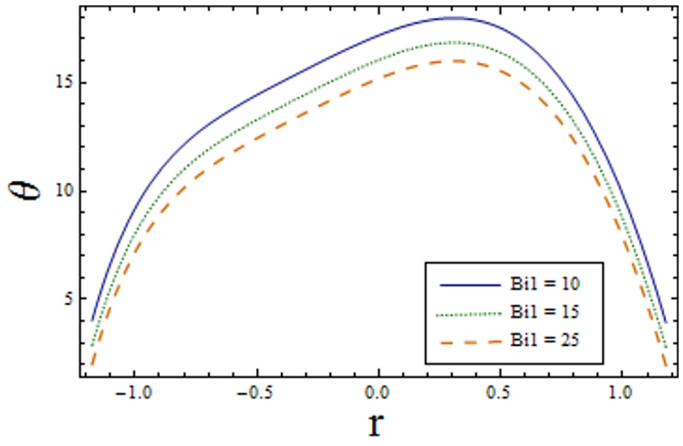

Fig 13. Variation of Bi_1 on θ when $\epsilon = 0.2$, x = 0.3, t = 0.1, $E_1 = 0.04$, $E_2 = 0.03$, $E_3 = 0.02$, α = 1.5, H = 2.0, β = 0.7 and k = 3.5.

doi:10.1371/journal.pone.0156995.g013

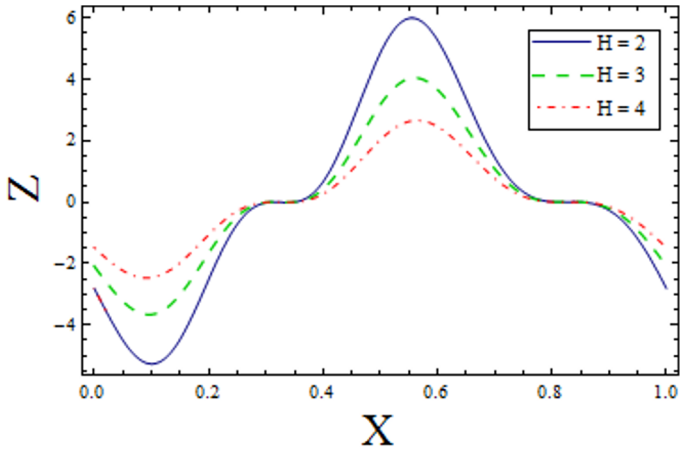

Fig 14. Variation of H on Z when $\epsilon = 0.2$, t = 0.1, Br = 2, $E_1 = 0.04$, $E_2 = 0.03$, $E_3 = 0.02$, α = 1.5, β = 0.7, Bi_1 = 10 and k = 4.

doi:10.1371/journal.pone.0156995.g014

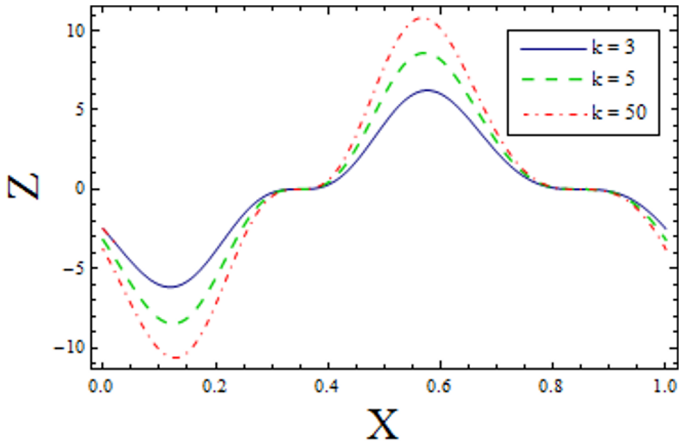

Fig 15. Variation of k on Z when $\epsilon = 0.2$, t = 0.1, Br = 2, $E_1 = 0.04$, $E_2 = 0.03$, $E_3 = 0.1$, α = 1.5, β = 0.7, Bi_1 = 5, H = 2.

doi:10.1371/journal.pone.0156995.g015

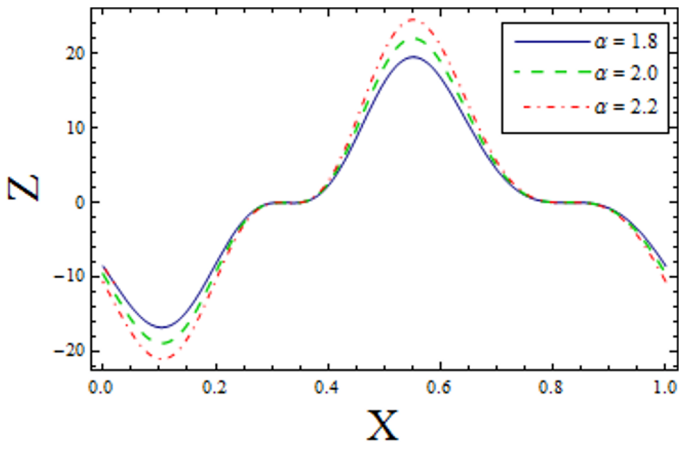

Fig 16. Variation of α on Z when $\epsilon = 0.2$, t = 0.1, Br = 2, $E_1 = 0.04$, $E_2 = 0.03$, $E_3 = 0.1$, H = 1.5, $\beta = 0.7$, $Bi_1 = 5$ and k = 3.5.

doi:10.1371/journal.pone.0156995.g016

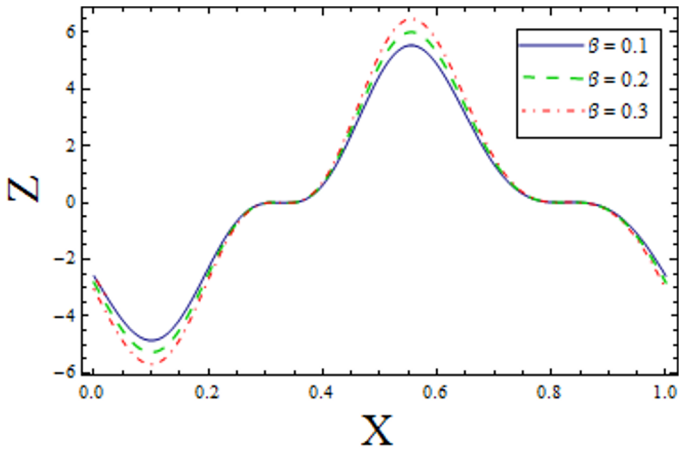

Fig 17. Variation of β on Z when $\epsilon = 0.2$, t = 0.1, Br = 2, $E_1 = 0.04$, $E_2 = 0.03$, $E_3 = 0.1$, $\alpha = 1.5$, H = 2, $Bi_1 = 5$ and k = 3.5.

doi:10.1371/journal.pone.0156995.g017

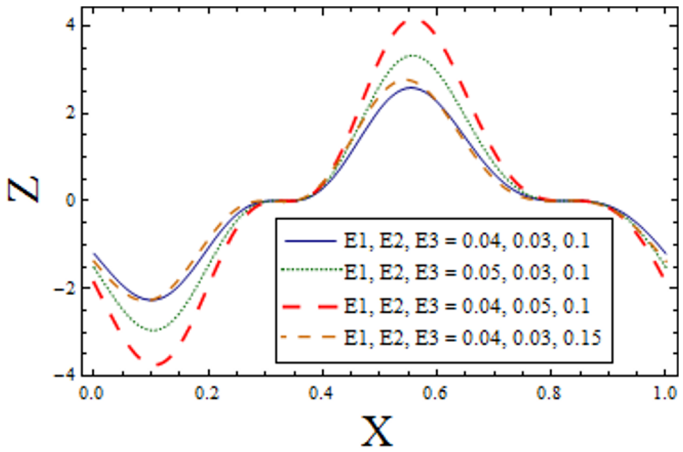

Fig 18. Variation of *complaint wall parameters* on Z when $\epsilon = 0.2$, t = 0.1, Br = 2, H = 02, $\alpha = 1.5$, $\beta = 0.7$, $Bi_1 = 10$ and k = 0.5.

doi:10.1371/journal.pone.0156995.g018

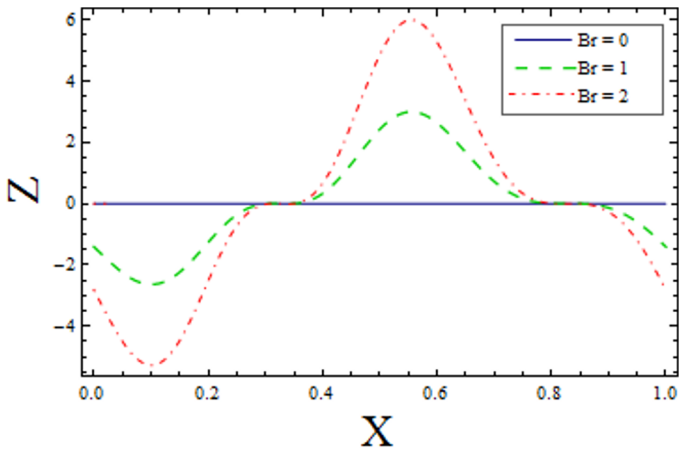

Fig 19. Variation of *Br* on *Z* when $\epsilon = 0.2$, t = 0.1, H = 2, $E_1 = 0.04$, $E_2 = 0.03$, $E_3 = 0.1$, α = 1.5, β = 0.7, Bi_1 = 10 and k = 3.5.

doi:10.1371/journal.pone.0156995.g019

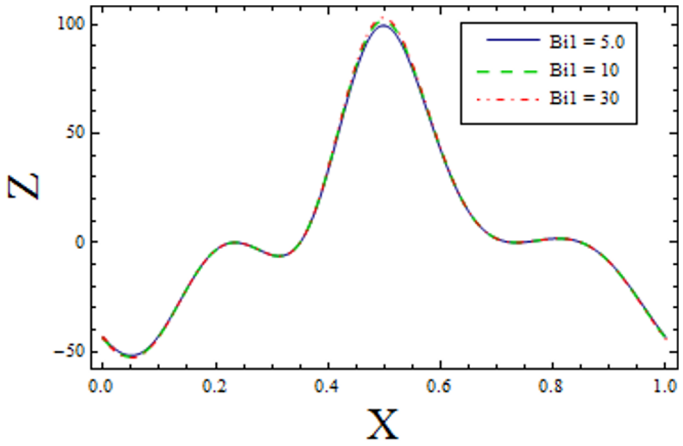

Fig 20. Variation of Bi_1 on *Z* when $\epsilon = 0.2$, t = 0.1, H = 2, $E_1 = 0.04$, $E_2 = 0.03$, $E_3 = 0.1$, α = 1.5, β = 0.7, Br = 2, H = 2 and k = 3.5.

doi:10.1371/journal.pone.0156995.g020

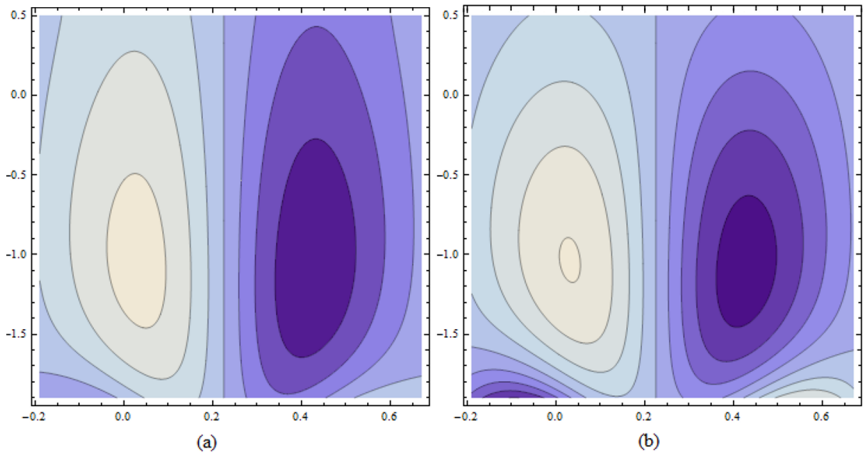

Fig 21. Variation of *H* on *ψ* for $E_1 = 0.02$, $E_2 = 0.01$, $E_3 = 0.03$, α = 0.2, β = 0.02, $\epsilon = 0.2$, t = 0.0, k = 3.5 when (a): H = 0.8 and (b): H = 1.1.

doi:10.1371/journal.pone.0156995.g021

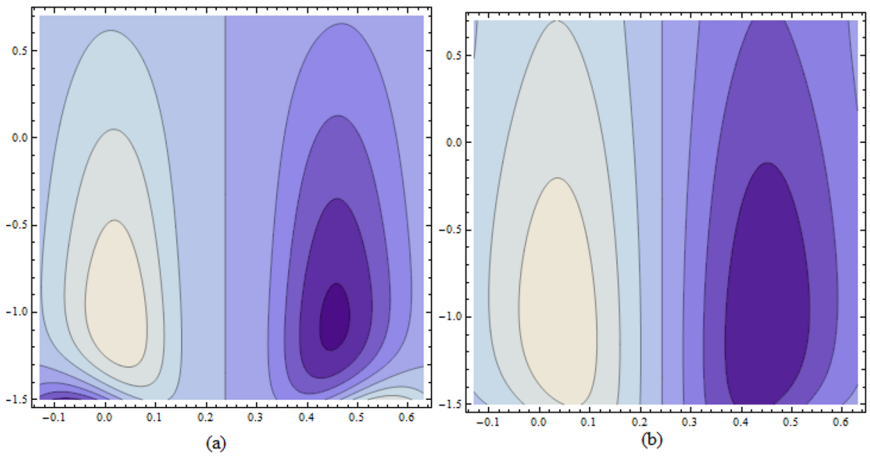

Fig 22. Variation of *k* on *ψ* for $E_1 = 0.02$, $E_2 = 0.15$, $E_3 = 0.05$, $\alpha = 0.2$, $\beta = 0.02$, $\epsilon = 0.2$, $t = 0.0$, $H = 0.8$ when (a): $k = 3.8$ and (b): $k = 5$.

doi:10.1371/journal.pone.0156995.g022

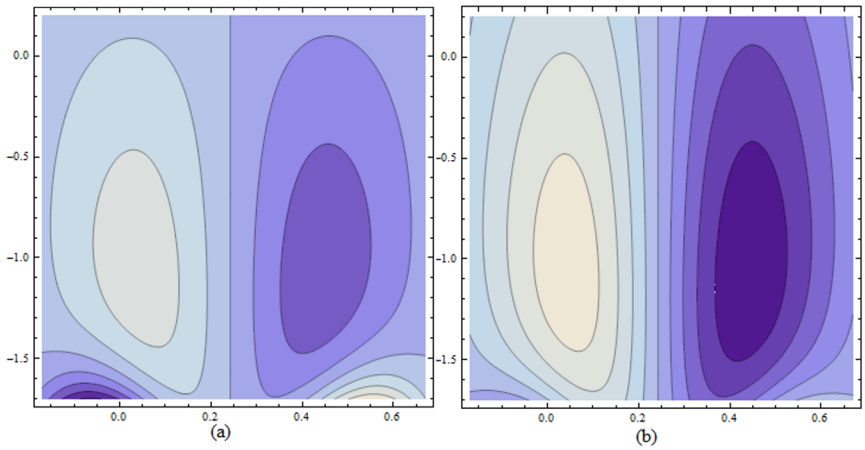

Fig 23. Variation of *α* on *ψ* for $E_1 = 0.02$, $E_2 = 0.15$, $E_3 = 0.05$, $k = 3.5$, $\beta = 0.02$, $\epsilon = 0.2$, $t = 0.0$, $H = 2.0$ when (a): $\alpha = 0.5$ and (b): $\alpha = 1.1$.

doi:10.1371/journal.pone.0156995.g023

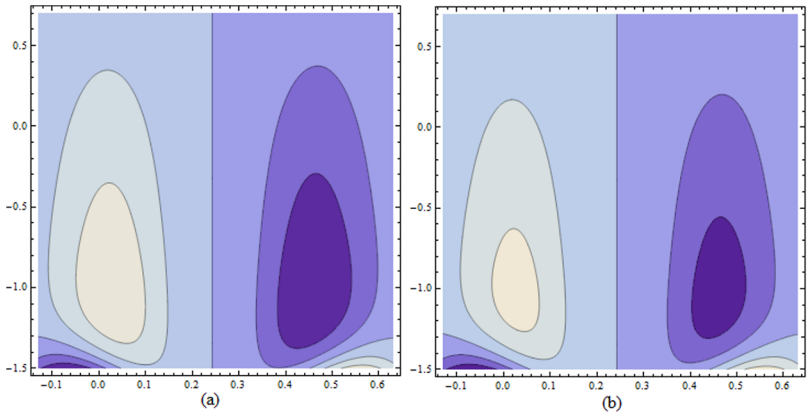

Fig 24. Variation of *β* on *ψ* for $E_1 = 0.02$, $E_2 = 0.15$, $E_3 = 0.05$, $\alpha = 0.7$, $k = 3.5$, $\epsilon = 0.2$, $t = 0.0$, $H = 2.0$ when (a): $\beta = 0.3$ and (b): $\beta = 1.5$.

doi:10.1371/journal.pone.0156995.g024

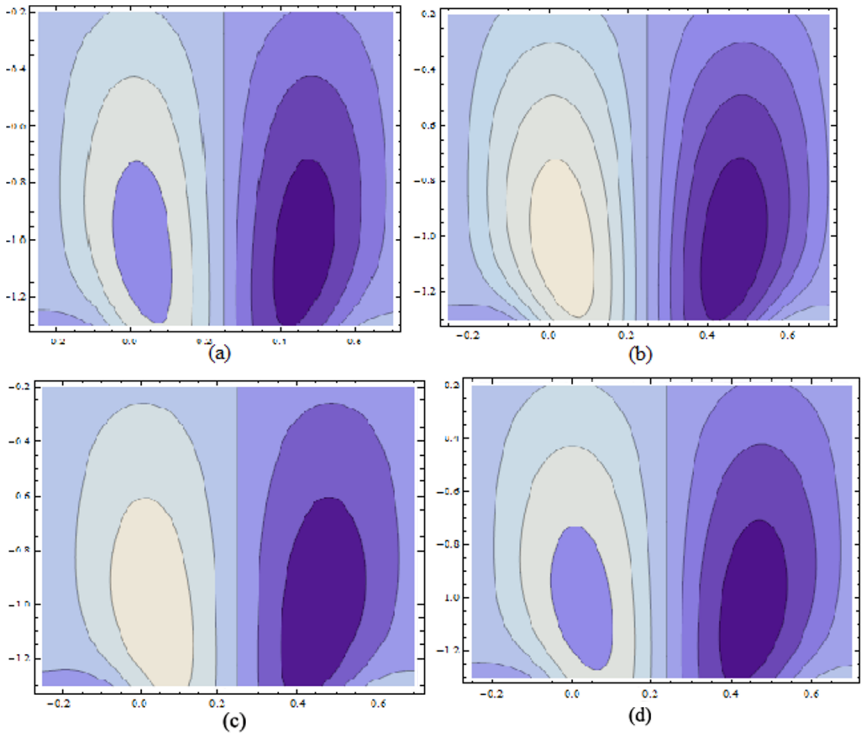

Fig 25. Variation of *wall properties* on ψ for H = 5, α = 1.5, k = 3.5, ϵ = 0.2, t = 0.0, β = 0.4 when (a): E_1 = 0.03, E_2 = 0.02, E_3 = 0.1 (b): E_1 = 0.04, E_2 = 0.02, E_3 = 0.1 (c): E_1 = 0.03, E_2 = 0.04, E_3 = 0.1 and (d): E_1 = 0.03, E_2 = 0.02, E_3 = 0.2.

doi:10.1371/journal.pone.0156995.g025

noticed for increased H. Fig 22a and 22b show the effect of curvature parameter k on the streamlines. These figures show that the bolus size enhances for larger K. Fig 23a and 23b illustrate the fact that the trapped bolus size increases when fluid parameter α is enhanced. Number of streamlines are more. Fig 24a and 24b show that size of trapped bolus decreases when we increase the values of fluid parameter β. We have analyzed through Fig 25a–25d that the streamlines increases through the increase in elastic parameters E_1 and E_2 while increase in E_3 has no show significant effect. Moreover, by taking $\alpha = \beta = H = Bi_1 = 0$ results can be obtained for viscous case [24].

Conclusions

Peristaltic motion of MHD Prandtl Eyring fluid flowing through curved geometry is discussed. Walls of channel are chosen to be compliant. Heat transfer phenomenon is also analyzed. Main findings of this study are:

1. Symmetry of velocity profile about the centre line is disturbed for the flow in curved channel.
2. The velocity profile has decreasing behavior for increasing values of Hartman number H.
3. Temperature profile is a decreasing function of Biot number Bi_1.
4. The absolute value of heat transfer coefficient for planer channel is higher than the curved one.
5. Size of trapped bolus increases for α but it decreases via β.

Author Contributions

Conceived and designed the experiments: TH SB FA MR. Performed the experiments: TH SB FA MR. Analyzed the data: TH SB FA MR. Contributed reagents/materials/analysis tools: TH SB FA MR. Wrote the paper: TH SB FA MR.

References

1. Latham T. W., Fluid motion in a peristaltic pump, MS thesis, MIT, Cambridge, AMA (1966).
2. Shapiro A. H., Jaffrin M. Y. and Weinberg S. L., Peristaltic pumping with long wave-lengths at low Reynolds number, J Fluid Mech (1969); 37(4): 799–25.
3. Gul T., Islam S., Ali Shah R., Khan I. and Shafie S., Thin film flow in MHD third grade fluid on a vertical belt with temperature dependent viscosity, (2014); 9(6): e97552.
4. Gul T., Islam S., Ali Shah R., Khan I., Khalid A. and Shafie S., Heat transfer analysis of MHD thin film flow of an unsteady second grade fluid past a vertical oscillating belt, (2014); 9(11): e103843.
5. Gul T., Islam S., Ali Shah R., Khalid A., Khan I. and Shafie S., Unsteady MHD thin film flow of an Oldroyd-B fluid over an oscillating inclined belt, (2015); 10(7): e0126698.
6. Ellahi R., The effects of MHD and temperature-dependent viscosity on the flow of non-Newtonian nanofluid in a pipe: Analytical solutions, Appl Math Model (2013); 37(3): 1451–57.
7. Lachiheb M., Effect of coupled radial and axial variability of viscosity on the peristaltic transport of Newtonian fluid, Appl Math Comput (2014); 244: 761–71.
8. Saleem M. and Haider A., Heat and mass transfer on the peristaltic transport of non-Newtonian fluid with creeping flow, Int J Heat Mass Transfer (2014); 68: 514–26
9. Vajravelu K., Radhakrishnamacharya G. and Radhakrishnamurty V., Peristaltic flow and heat transfer in a vertical porous annulus with long wave approximation, Int J Nonlinear Mech (2007); 42(5): 754–59.
10. Javed M., Hayat T. and Alsaedi A., Peristaltic flow of Burgers' fluid with compliant walls and heat transfer, Appl Math Comput (2014); 244: 654–71.
11. Nadeem S., Hayat T., Akbar N. S., Malik M. Y., On the influence of heat and mass transfer in peristalsis with variable viscosity, Int J Heat Mass Transfer (2009); 52: 4722–30.
12. Hina S., Hayat T., Asghar S. and Hendi A. A., Influence of complaint walls on peristaltic motion with heat/mass transfer and chemical reactions, Int J Heat Mass Transfer (2012); 55: 3386–94.
13. Srinivas S., Gayathri R. and Kothandapani M., The influence of a slip conditions, wall properties and heat transfer on MHD peristaltic transport, Comput Phys Comm (2009); 180: 2115–22.
14. Mekheimer Kh.S., Salem A.M. and Zaher A. Z., Peristaltically induced MHD slip flow in a porous medium due to a surface acoustic wavy wall, J Egyptian Math Soc (2014); 22: 143–51.
15. Abd Elmaboud Y. and Mekheimer Kh. S., Nonlinear peristaltic transport of second order fluid through a porous medium, Appl Math Model (2011): 35(6): 2695–10.
16. Tripathi D., Study of transient peristaltic heat flow through a finite porous channel, Math Comput Model (2013); 57(5–6): 1270–83.
17. Kothandapani K. and Prakash J., Effect of radiation and magnetic field on peristaltic transport of nanofluids through a porous space in a tapered asymmetric channel, J Magn Magn Mater (2015); 378: 152–63.
18. Sinha A., Shit G. C. and Ranjit N. K., Peristaltic transport of MHD flow and heat transfer in an asymmetric channel: Effects of variable viscosity, velocity slip and temperature jump, Alex Eng J (2015); 54(3): 691–04.
19. Gad N. S., Effects of Hall current on peristaltic transport with compliant walls, Appl Math Comput (2014); 235: 546–54.
20. Abd-Alla A. M., Abo-Dahab S. M. and El-Shahrany H. D., Influence of heat and mass transfer, initial stress and radially varying magnetic field on the peristaltic flow in an annulus with gravity field, J Mag Magn Mater (2014); 363: 166–78.
21. Abd-Alla A. M. and Abo-Dahab S. M., Magnetic field and rotation effects on peristaltic transport of a Jeffrey fluid in an asymmetric channel, J Mag Magn Mater (2015); 374: 680–89.
22. Sato H., Fujita T. and Okabe M., Two dimensional peristaltic flow in a curved channels, Trans Jpn Soc Mech Eng (2000); 66(643): 679–85.
23. Hayat T., Ali N. and Sajid M., Long wavelength flow analysis in a curved channel, Z Naturforsch (2010); 65(3): 191–96.

24. Hayat T., Javed M. and Hendi A. A., Peristaltic transport of viscous fluid in a curved channel with compliant walls, Int J Heat Mass Transfer (2011); 54(7–8): 1615–21.

25. Ali N, Sajid M., Abbas Z. and Javed T., Non-Newtonian fluid flow induced by peristaltic waves in a curved channel, European J Mechi-B/Fluids (2010); 29(5): 387–94.

26. Abbasi F.M., Hayat T. and Alsaedi A., Numerical analysis for MHD peristaltic transport of Carreau-Yasuda fluid in a curved channel with Hall effects, J Magn Magn Mater (2015); 382: 104–10.

27. Hina S., Mustafa M., Hayat T. and Alotaibi N. D., On Peristaltic motion of pseudoplastic fluid in a curved channel with heat/mass transfer and wall properties, Appl Math Comput (2015); 263: 378–91.

28. Hina S., Hayat T. and Alsaedi A., Heat and mass transfer effects on the peristaltic flow of Johnson-Segalman fluid in a curved channel with compliant walls, Int J Heat Mass Transfer (2012); 55(13–14): 3511–21.

29. Hayat T., Hina S., Hendi A. A. and Asghar S., Effects of wall properties on the peristaltic flow of third grade fluid in a curved channel with heat and mass transfer, Int J Heat Mass Transfer (2011); 54: 5126–36.

30. Hayat T., Yasmin H., Alhuthali M. S. and Kutbi M. A., Peristaltic flow of a non-Newtonian fluid in an asymmetric channel with convective boundary conditions, J Mech (2013); 29(4): 599–07.

31. Hayat T., Yasmin H., Ahmed B. and Chen B., Simultaneous effects of convective conditions and nanoparticles on peristaltic motion, J Mol Liq (2014); 193: 74–82.

32. Hussain Q., Hayat T., Asghar S. and Alsulami H., Mixed convective peristaltic transport in a vertical channel with Robin's condition, J Braz Soc Mech Sci Eng (2014); 36(4): 681–95.

33. Hussain Q., Hayat T., Asghar S. and Alsaedi A., Heat transfer in a porous saturated way channel with asymmetric convective boundary conditions, J Central South University (2015); 22(1): 392–01.